Journal of Computer-Aided Molecular Design, 2 (1988) 281–309
ESCOM

J-CAMD 050

Molecular mechanics calculations on deaminooxytocin and on deamino-arginine-vasopressin and its analogues

A. Liwo, A. Tempczyk and Z. Grzonka*

Institute of Chemistry, University of Gdansk, ul. Sobieskiego 18, 80-952 Gdansk, Poland

Received 7 March 1988
Accepted 10 June 1988

Key words: Molecular mechanics; Conformational analysis; Neurohypophyseal hormones; Oxytocin and vasopressin analogues; Cyclic moiety

SUMMARY

The backbone conformations of the cyclic moieties of 1-[β-mercaptopropionic acid]-oxytocin ([Mpa^1]-OT), [1-β-mercaptopropionic acid]-arginine-vasopressin ([Mpa^1]-AVP), [1-(β′-mercapto-β,β-cyclopentamethylene)propionic acid]-arginine-vasopressin ([Cpp^1]-AVP), and [1-thiosalicylic acid]-arginine-vasopressin ([Ths^1]-AVP) have been analyzed by means of molecular mechanics. In these calculations, the side chains were simulated by pseudoatoms. For the three last compounds, the calculations were also performed on the whole molecules, in order to shed light on the differences in their biological activity. Their starting conformations were obtained by attaching the acyclic tail and side chains to the lowest energy conformations of the cyclic parts. In the case of [Ths^1]-AVP, however, other starting conformations were also examined, which were obtained by attaching the planar benzene ring to the lowest energy conformations of [Mpa^1]-AVP. In the calculations, all the degrees of freedom were relaxed and Weiner's force field was used, the parameters required for the benzene parts of [Ths^1]-AVP being determined from the experimental data available, as well as from the results of molecular dynamics calculations on the model compounds. The lowest energy conformations of [Mpa^1]-AVP and [Cpp^1]-AVP are similar, while [Ths^1]-AVP differs from them near the disulphide region, due to the presence of a planar benzene ring. Interactions involving the charged guanidine group of arginine make, in each case, an important contribution to the conformational energy. A model description of the shapes of the oxytocin and vasopressin ring has been proposed, which is based on the cyclohexane geometry. This description is in good correlation with the energetics of the conformations corresponding to different shapes.

INTRODUCTION

Many conformational studies have been carried out on vasopressin and oxytocin themselves and on their derivatives, in which both theoretical and experimental methods have been used [1,2]. Because of the high complexity of the compounds under study, the theoretical methods are limit-

* To whom correspondence should be addressed.

ed to employing certain empirical force fields. Such force fields can be used in the molecular mechanics method (energy minimization) when we are interested only in obtaining the energy minima, in the Monte Carlo or related methods when certain statistical averages are needed, or in the molecular dynamics method when the time evolution of a system is required [3]. Experimental investigations in conformations employ mainly NMR and CD techniques.

In the case of oxytocin (OT), extensive molecular mechanics studies have been performed by Nikiforovich et al. [4] and Spasov and Popov [5]. Both groups of authors used rigid valence geometry (i.e., only the torsion angles except for ωs, owing to the assumed rigidity of the peptide bond were optimized) and the united-atom approximation (all the hydrogens except for those able to form the hydrogen bonds were fused to heavy atoms). Spasov and Popov used the force field and valence geometries of Momany et al. [6], while Nikiforovich et al. used the nonbonded potentials of Dashevskii [7], the charges of Momany et al., and the valence geometries of Deslauriers et al. [8]. As far as the lowest energy conformation is concerned, there are no substantial differences in the results obtained by either group, while the next conformations differ more in both geometry and energy relations. This may result from the differences in the force fields applied and/or in the procedure of generating the initial approximations.

Molecular mechanics calculations have also been carried out on arginine-vasopressin (AVP) [9,10], mesotocin (MT) and vasotocin (VT) [10]. Generally, the lowest energy conformations obtained are similar to that of oxytocin.

As yet, there are few crystallographic data on the hypophyseal hormones because these compounds have proved difficult to crystallize. Studies on deaminooxytocin have been carried out by Blundell et al. [11] and Wood et al. [12]. The latter have revealed the presence of at least two conformers in the crystal structure, both of which possess one type II β-turn in the Ile^3-Gln^4 region of the cyclic moiety and one type III β-turn in the Pro^7-Leu^8 region of the tail. Langs et al. [13] investigated the crystal structure of the pressinoic acid (the cyclic moiety of arginine-vasopressin). They have found only one backbone conformation with a distorted II′ β-bend in the Phe^3-Gln^4 region and one type I β-turn in the Gln^4-Asn^5 region.

One purpose of the present work was to investigate and describe the conformational space of deaminooxytocin and some selected arginine-vasopressin derivatives by means of molecular mechanics. These calculations are the first part of our extensive conformational studies designed to explain the difference in the biological activity of neurohypophyseal hormones and their analogues. Because the cyclic moiety of these compounds is much more rigid than the acyclic tail, we have investigated this first. Detailed calculations on the whole molecules have been performed on [1-β-mercaptopropionic acid]-arginine-vasopressin ([Mpa^1]-AVP), [1-(β'-mercapto-β,β-cyclopentamethylene)propionic acid]-arginine-vasopressin ([Cpp^1]-AVP), and [1-thiosalicylic acid]-arginine-vasopressin ([Ths^1]-AVP) which differ from the parent hormone, AVP, in the first residue, which is cysteine in the case of arginine-vasopressin, β-mercaptoproprionic acid in the case of [Mpa^1]-AVP, β'-mercapto-β,β-cyclopentamethylenepropionic acid in the case of [Cpp^1]-AVP, and thiosalicylic acid for [Ths^1]-AVP. [Mpa^1]-AVP has antidiuretic activity five times higher than that of AVP, exhibiting at the same time similar pressor activity [14]. [Cpp^1]-AVP is a strong antagonist of the pressor response and, on the other hand, has hardly any antidiuretic activity [15]. On the contrary, [Ths^1]-AVP does not exhibit antagonistic activity and its agonistic activity is very low [16]. There are also substantial differences in the affinity of these compounds to the vasopressor receptors V_1 and V_2. In the case of [Cpp^1]-AVP, the affinity to the V_1 receptor is the same as

that of vasopressin, while for [Ths^1]-AVP it is 36 times lower. In the case of the V_2 receptor, these affinities are 65 and 1200 times lower, respectively [17].

METHODS

We applied the force field of Weiner et al. [18], which is designed for the calculations on peptides and nucleotides. The united-atom approximation was applied and all degrees of freedom were assumed to be relaxed. Relaxing all degrees of freedom offers the advantage of including such effects as the distortion of the bonds and valence angles which is very often important to reflect well the energy relations between the conformers (for example, the X-H bonds are often remarkably lengthened on forming the hydrogen bonds). However, this considerably increases the number of adjustable variables (for [Cpp^1]-AVP there are 300 independent variables to be optimized) and requires additional parameters like bond and bond angle constants when compared to constrained molecular mechanics.

In the force field used, the energy of a system is expressed by Eq. (1) (see Ref. 18).

$$E = \sum_{\text{bonds}} k_i^{\,d}\,(d_i - d_i^{\circ})^2 + \sum_{\text{bond angles}} k_\theta(\theta_i - \theta_i^{\circ})^2 + \sum_{i<j} q_i q_j/\varepsilon r_{ij} + \sum_{\substack{i<j \\ \text{except for H bonds}}} \varepsilon_{ij}[(r_{ij}^{\circ}/r_{ij})^{12}$$

$$- 2(r_{ij}^{\circ}/r_{ij})^6] + \sum_{\substack{i<j \\ \text{H bonds}}} (C_{ij}/r_{ij}^{12} - D_{ij}/r_{ij}^{10}) + \sum_{\text{torsion angles}} [\tfrac{1}{2}V_i^{1}\cos(\omega_i) - \tfrac{1}{2}V_i^{2}\cos(2\omega_i)$$

$$+ \tfrac{1}{2}V_i^{3}\cos(3\omega_i)]$$

$$\varepsilon_{ij} = (\varepsilon_i\varepsilon_j)^{\frac{1}{2}},\ r_{ij}^{\circ} = \tfrac{1}{2}(r_i^{\circ} + r_j^{\circ}) \qquad (1)$$

where d° and θ° denote strainless values of the bond lengths and bond angles, $k_i^{\,d}$ and k_θ are the respective force constants q_i is the charge on the *i*th atom, r_{ij} is the distance between *i*th and *j*th atoms, ε_i and r_i° are the van der Waals well-depth and radius of atom, i, V^1, V^2, and V^3 are the torsional constants.

The first two sums represent bonds and bond angle distortion and the next three sums stand for the electrostatic and van der Waals (VDW) energy. In these sums, atoms i and j are not bonded and have no common atom bonded to them. As shown, the electrostatic energy is represented by the interactions of point charges centered on atoms. For most of the VDW interactions, the Lennard-Jones (6–12) potential is used, while for atoms directly involved in H-bonds the potential is of the 10–12 type, which provides against unreasonably long H-bonds. We have chosen the distance-dependent dielectric constant ($\varepsilon = r_{ij}$). According to the paper of Weiner et al. [18], this simulates the effect of the solvent. Therefore, the results of our calculations are closer to the results of calculations with explicit inclusion of solvent effect than to those in vacuo. Also according to the procedure of Weiner et al., we scaled down the 1,4 electrostatic and VDW interactions energies by a factor of 0.5.

For the interaction energy of 1,4-nonbonded atoms, the electrostatic plus VDW approximation is not sufficient (because of the effects arising from bond–bond interactions) and, therefore, the residue is expanded into the Fourier series in the respective torsion angles to give the torsional energy. In the force field applied, there is also another kind of torsional energy corresponding to 1,3-

nonbonded atoms interactions. For atom B having three substituents A, C, and D, we define the so-called *improper* torsional angles A-B-C-D, A-B-D-C, C-B-A-D, C-B-D-A, D-B-A-C, and D-B-C-A. If the 'central' atom B is, for example, the carbonyl carbon, the respective contribution to the torsional energy represents the strain of the carbonyl group. In other force fields, such effects are described by introducing the out-of-plane bends. The second purpose of using the *improper* torsion angles is to keep the asymmetric carbons from racemization, when one uses the united-atom approximation.

We have modified the program MM2 of Allinger and Yuh [19] in order to adapt it to the force field used. Because we have found Allinger's original minimization procedure, which has in general first-order convergence, to converge very slowly and not always to a real minimum in the case of larger molecules, we have incorporated the Davidon-Fletcher-Powell second-order procedure [20].

Molecular mechanics parameters

In the cases of [Mpa^1]-AVP and [Cpp^1]-AVP, it was possible to take almost all the parameters directly from Ref. 18. For [Cpp^1]-AVP, we had only to estimate the charges on the cyclohexane ring. Because of their low values, we simply distributed the charges on the respective pseudoatoms according to CNDO/2D populations calculated for the model compound methylcyclohexyldisulphide so as to retain the charge of the whole system.

Because of the presence of the benzene ring incorporated into the peptide backbone for [Ths^1]-AVP, there were some unknown bonds, bond angles, and torsional constants and charges. They have been estimated partially on the basis of the experimental data and partially on the basis of the results of the published and our own quantum mechanical calculations. To facilitate later considerations, the types of atoms used in the calculations are given below:

C: carbonyl carbon not connected with an aromatic ring.
CA: aromatic carbon with one substituent.
CB: carbonyl carbon explicitly connected with an aromatic ring.
CD: aromatic carbon with one hydrogen.
CT: aliphatic carbon with four substituents.
C2: methylene group.
C3: methyl group.
N: amide nitrogen.
N2: guanidine nitrogen.
H: amide hydrogen.
HO: hydroxyl hydrogen.
H3: guanidine hydrogen.
O: carbonyl oxygen.
OH: hydroxyl oxygen.
S: sulphur.
LP: lone pair.

Explicit lone pairs with a 'bond length' of 0.679 Å and 'bond angle' of 96.7° were used only in the case of sulphur. We have also found that, in the case of the disulphide bridge, including LP-LP electrostatic interactions causes considerable lengthening (up to 2.08 Å) of the disulphide bond,

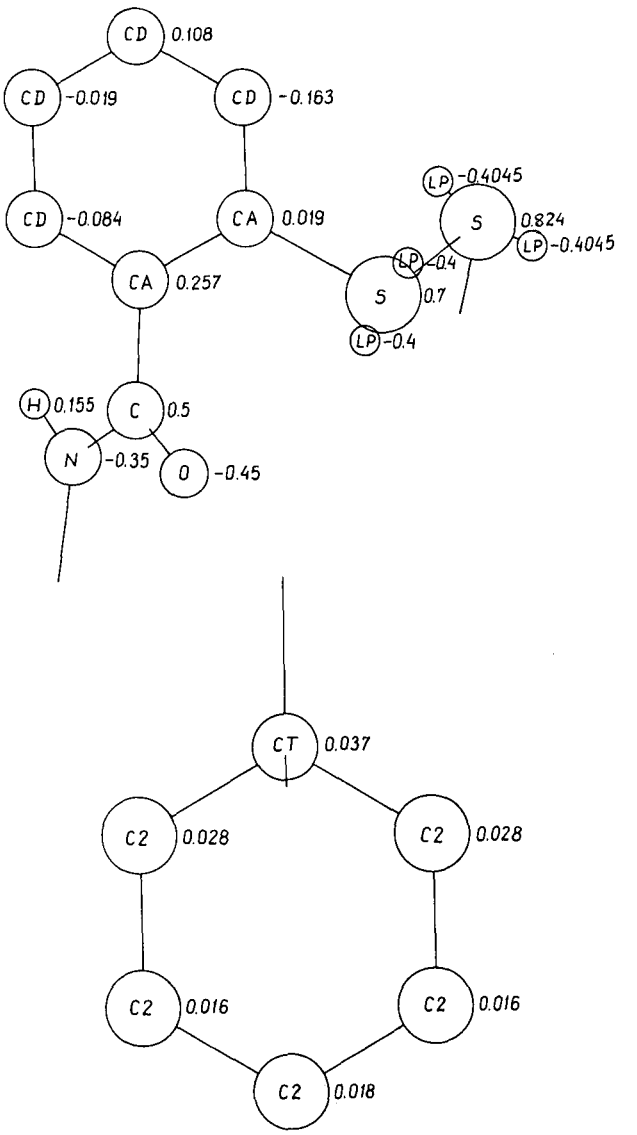

Fig. 1. Charges of the aromatic fragment of the cyclic part of the [Ths^1]-AVP and cyclohexyl fragment of [Cpp^1]-AVP used in molecular mechanics calculations.

which could be compensated only by taking an unreasonably short strainless S-S bond length. Therefore we have excluded these interactions, as well as other interactions of lone pairs with other atoms 1,4-nonbonded to them.

To estimate the molecular mechanics parameters of the aromatic part of the backbone of [Ths^1]-AVP, we first chose several model compounds for which we could find the relevant experimental data or perform quantum mechanical calculations. These were benzamide, *N*-methylbenz-

amide, benzenethiol, phenyl disulphide, methylphenyl disulphide, and [2-carboxamidophenyl]-disulphide.

The charges on the aromatic amide and disulphide group were estimated by calculating the molecular electrostatic potential of benzamide and phenyl disulphide from the CNDO/2D wave function and then fitting the charges, by means of a least-squares method, so as to approximate the potential. For each compound, the potential was calculated at about 200 points for variously oriented planes. The distance of a point from the molecule was about 4 Å. We found that at such a distance the potential is well represented by the set of point charges centered on atoms, being at the same time large enough to allow for determining the charges. For most points the differences between the CNDO/2 and the charge potential were about 5%, in extreme cases about 15%. The standard deviations in charges were not greater than 0.08 e.

To compare the compatibility of charges thus determined and the charges of Weiner et al. [18] which were obtained from the ab initio wave functions, we performed the same calculations on *N*-methylacetamide. We found that, in this case, the CNDO/2D potential gives greater carbonyl carbon and lower in its absolute value amide nitrogen charge, when compared with the charges obtained by Weiner et al. (0.764 e instead of 0.526 e and -0.391 e instead of -0.52 e, respectively). Therefore, for the aromatic amide part we corrected the charges on C and N so as to reproduce this tendency. Finally, the aromatic amide and disulphide charges have been adjusted so as to reproduce the experimental dipole moments of benzamide and diphenyl disulphide, at the same time satisfying the electroneutrality condition. Finally, we calculated the charges on the aromatic ring of [Ths^1]-AVP by taking the model compound [2-carboxamidophenyl]-disulphide. In this calculation we fixed the charges on the disulphide and amide group and estimated only the charges on the ring. Final charges for the aromatic part of [Ths^1]-AVP and on the cyclohexyl ring of [Cpp^1]-AVP are given in Fig. 1.

The VDW constants for both 6–12 and 10–12 potential have been taken directly from Ref. 18. For the CB atom, we assumed the same constants as for the ordinary carbonyl carbon, i.e. $\varepsilon = 0.12$ kcal/mol and $r^\circ = 1.85$ Å.

To estimate the torsional constants of the rotation about the aromatic amide bond we performed MNDO calculations on *N*-methylbenzamide, varying the ω angle. In the case of the rotation about the CA-S bond we performed CNDO/2 calculations on methylphenyldisulphide, while in the case of the rotation about the CA-CB bond of benzamide we used the results of the NDDO calculations of Hoffman and Birner [21], because both CNDO/2 and MNDO fail to reproduce the energetics of the rotation about this bond [21]. In all cases, we subtracted the electrostatic and VDW terms from the total energy and fitted the sum of cosines to the residue by means of a least-squares method. We found, however, that applying this procedure to *N*-methylacetamide gives too low a value of the twofold rotational constant, when compared with the work of Weiner et al. [18]. Therefore, we scaled the twofold torsional constant of the aromatic amide bond by the ratio of Weiner's and the MNDO barrier of *N*-methylacetamide. To improve the CA-S bond torsional constants of aromatic disulphides we used the NMR rotational barrier of benzenethiol [22]. From this barrier and from CNDO/2D potential charges we calculated the twofold 'experimental' torsional constant of this compound, then we calculated it using the results of CNDO/2 calculations. Scaling the twofold torsional constant of methylphenyldisulphide by the ratio of the 'experimental' and theoretical constant obtained for benzenethiol gave the 'improved' constants of the rotation about the CA-S bond in [Ths^1]-AVP. Other unknown torsional constants have been

taken by extrapolation from the work of Weiner et al. [18]. The torsional constants are summarized in Table 1.

The missing (i.e., not given in the paper of Weiner et al. [18]) bond and bond angle constants have been taken from the data on similar compounds (Refs. 18 and 23) and are given in Tables 2 and 3. Some of them have been corrected to give the best fit between the experimental and calculated geometries and IR spectra of *N*-methylbenzamide and diphenyldisulphide (see Tables 4 and 5).

CALCULATIONS

Conformational calculations consisted of two steps. First, we examined the backbone structures of the cyclic parts of deaminooxytocin and the vasopressin analogues studied. Based on the lowest energy conformations thus obtained, we performed calculations on the whole molecules of the vasopressin analogues. In the case of [Cpp[1]]-AVP, however, we omitted the first step because, according to preliminary geometric considerations, the cyclohexane ring should not greatly disturb the structure of the backbone.

In the first step, all side chains, except for those of cysteines, were simulated by pseudoatoms with bond-stretching constants of 100 kcal/Å^2 and bending constants of 10 kcal/deg^2. Such low

TABLE 1
TORSIONAL CONSTANTS

Angle type	V_1	V_2	V_3
		(kcal/mol)	
(a) General[a]			
X-CA-CA-X	0	10.6	0[b]
X-CA-CB-X	0	3.0	0[c]
X-CB-N-X	0	12.36	0[d]
(b) Specific			
CA-CA-S-S	0	0.7	0[e]
CD-CA-S-S	0	0.7	0[e]
CA-CA-S-LP	0	0	0[b]
CD-CA-S-LP	0	0	0[b]
O-CB-N-H	1.5	4.12	0[d]
(c) Improper			
O-CB-X-X	0	21.0	0[b]

[a]In the case of the *general* parameters the symbol X stands for *all* atoms bonded to the atom indicated, so the corresponding torsional constants refer to the sum over *all* angles of a given central axis and are therefore divided by the number of angles to obtain the constants corresponding to a particular angle, while the *specific* parameters refer to a given angle. For an explanation of the *improper* angles, see text.

[b]Values from Ref. 18 by extrapolation.

[c]Value obtained from the results of NDDO calculations of Hoffman and Birner [21].

[d]From the results of our MNDO calculations on *N*-methylbenzamide, see text.

[e]From the results of our CNDO/2 calculations on methylphenyl disulphide and NMR data on benzenethiol [22].

TABLE 2
BOND CONSTANTS

Bond type	d°(Å)	k_d(kcal/Å^2)
CA-CA	1.40	469[a]
CA-CB	1.49	317[b]
CA-S	1.81	222[c]
CB-N	1.34	490[b]
CB-O	1.249	525[b]

[a]Values from Ref. 18.
[b]From Ref. 23, corrected to reproduce the experimental geometry and vibrational frequencies of benzamide and *N*-methylbenzamide.
[c]From Ref. 18, corrected to the experimental data.

values, especially those of the bending constants, were assumed in order not to preserve rigorously the bond lengths and valence angles involving the pseudoatoms whose size and position vs. the respective residues should not be fixed due to the lability of the side chains. The 'bond lengths' and VDW radii of the pseudoatoms have been chosen according to the work of Crippen and Viswandhan [24]. The values of d° and r° were 4.0 Å for Tyr, 2.5 Å for Phe and Ile, 3.5 Å for Gln, and 2.5 Å for Asn, respectively. The strainless values of the valence angles have been fixed at 109.5°. In each case, we assumed the value of ε of 0.1 kcal/mol. The Cys^6 residue was blocked by the NMe_2 group.

The starting conformations were generated from 14 low-energy conformations of *cyclo*-(Cys-Ala)$_4$-Cys found by Spasov and Popov [5]. In the case of the [Mpa^1]-analogue, only some small corrections of the torsion angles φ and ψ were required to achieve the ring closure on the disulphide bond. This was done by means of a least-squares algorithm which was designed so as to cause minimal and uniform changes in the initial torsion angles (see the Appendix for a description of

TABLE 3
BOND ANGLE CONSTANTS

Angle type	θ°(deg)	k_θ(kcal/deg^2)
CA-CA-CD	120.0	130[a]
CA-CA-CB	120.0	25[a]
CA-CA-S	124.0	50[b]
CA-CB-N	116.0	50[a]
CA-CB-O	122.0	41[a]
CA-S-S	105.8	68[b]
CA-S-LP	95.7	600[b]
CB-CA-CD	120.0	25[a]
CB-N-CH	124.0	47[a]
CB-N-H	119.8	35[b]
N-CB-O	122.0	110[a]

[a]Values from Ref. 23.
[b]Values from Ref. 18 and from the experimental data on benzamide, *N*-methylbenzamide, and diphenyl disulphide.

TABLE 4

(A) COMPARISON OF THE CRYSTALLOGRAPHIC [29] AND CALCULATED VALUES OF SOME SELECTED BOND LENGTHS AND ANGLES OF BENZAMIDE

Bond	Length (Å)	
	Experimental	Calculated[a]
CB-N	1.342	1.340
CB-O	1.249	1.249
CA-CB	1.501	1.500

Angle	Value (deg)	
	Experimental	Calculated
CA-CB-N	117.5	117.4
CA-CB-O	120.5	121.7
N-CB-O	122.1	120.9

[a]In the calculations the structure of a dimer with two H-bonds has been assumed, according to the data of Blake and Small [29].

(B) COMPARISON OF THE EXPERIMENTAL AND CALCULATED FREQUENCIES OF BENZAMIDE AND *N*-METHYLBENZAMIDE

Vibration	Frequency (cm^{-1})	
	Experimental	Calculated
Amide I	1690[a]	1648
	1649[b]	1655
Amide II	1587[c]	1570
Amide III	1375[c]	1442
δ (NH_2)	791[d]	714
CA-N stretch	1304[a]	1377

[a]*N*-methylbenzamide; experimental data from Ref. 30.
[b]Benzamide; experimental data from Ref. 31.
[c]Benzamide; experimental data from Ref. 32.
[d]Benzamide; experimental data from Ref. 33.

TABLE 5
(A) COMPARISON OF THE CRYSTALLOGRAPHIC [34] AND CALCULATED VALUES OF SOME SELECTED BOND LENGTHS AND ANGLES OF DIPHENYL DISULPHIDE

Bond	Length (Å)	
	Experimental	Calculated[a]
S-S	2.03	2.04
CA-S	1.81	1.81

Angle	Value (deg)	
	Experimental	Calculated
CA-S-S	105.8	105.9
CD-CA-S	123.7	121.1

(B) COMPARISON OF THE EXPERIMENTAL AND CALCULATED IR FREQUENCIES OF DIPHENYL DISULPHIDE

Vibration	Frequency (cm^{-1})	
	Experimental	Calculated
S-S stretch	468[a], 512[b]	539.5
CA-S stretch	689[a]	696.4

[a]IR data of Cymerman and Willis [35].
[b]Raman data of van Wart and Scheraga [36].

the algorithm). In the case of the [Ths[1]]-analogue, however, because of the presence of the benzene ring, the changes were sometimes substantial and led to topologically different conformations.

For the starting conformations generated in such a way, energy minimization was then performed. Some selected torsion angles of the final conformations and their relative energies are summarized in Tables 6 and 7. The backbone structures are shown in Figs. 2 and 3.

It is worth noting that the lowest energy conformation of the cyclic part of AVP obtained by this procedure results from the conformation which in the case of oxytocin leads to the lowest energy conformation of the whole molecule [5], and in the case of AVP to the second lowest energy conformation [10]. We can therefore conclude that at least the energy relations of the conformations are well reproduced when the side chains are replaced by pseudoatoms.

To perform calculations on the whole molecules of the vasopressin analogues studied we combined, in each case, two of the lowest energy conformations of the cyclic part with the acyclic tail, whose backbone conformation was chosen after Spasov and Popov [10]. All the side chains were attached so as to avoid overlapping. We assumed the guanidine group of arginine to the proto-

TABLE 6
SELECTED TORSION ANGLES OF THE CONFORMATIONS OF THE CYCLIC PART OF [Mpa^1]-OT, [Mpa^1]-AVP, AND [Cpp^1]-AVP

		For the conformations shown in Fig. 2												
Energy (kcal/mol)		0.0	1.3	5.1	5.8	5.9	5.9	9.7	10.1	12.6	14.5	16.2	16.2	16.6	16.7
		Torsion angles (deg)[a]													
Mpa^1	ψ	(−155)	(−102)	(56)	(25)	(−86)	(70)	(81)	(−105)	(−164)	(77)	(107)	(160)	(−118)	(72)
(Cpp^1)	χ^1	56	−51	48	173	61	37	−68	49	−66	−63	163	171	180	50
	χ^2	59	164	68	57	−177	55	172	67	−76	−131	116	−173	177	175
	χ^3	−98	−71	−84	86	80	120	−104	155	96	81	−69	−89	−81	107
Tyr^2	φ	−84	−141	−58	−64	−56	44	48	−126	56	−164	−139	46	−96	−169
	ψ	67	69	−27	104	−34	40	37	127	28	128	137	45	−34	−171
Phe^3	φ	16	−146	−99	54	−103	62	−111	−41	−152	50	−38	75	−78	−56
(Ile^3)	ψ	−80	167	16	42	131	19	143	−43	113	35	−42	1	−23	−34
Gln^4	φ	−48	−54	−142	76	−57	−75	−56	−63	−34	55	−76	−73	−149	−108
	ψ	−38	−37	−178	−11	−32	80	121	−29	−53	26	−35	154	148	143
Asn^5	φ	−124	−85	−77	−81	−86	57	66	−95	−107	−69	176	−73	−75	−66
	ψ	39	−7	65	108	7	42	24	−46	43	−32	176	72	74	113
Cys^6	φ	−92	−173	−78	−95	−100	−165	−63	−136	−71	−99	−161	−85	−61	−86
	ψ	117	100	121	112	109	156	126	114	120	111	143	114	123	126
	χ^1	168	−171	−178	−71	167	61	170	49	173	−57	−176	−88	−71	74
	χ^2	162	−63	−175	−61	−138	81	−171	88	122	87	159	162	146	−125
	χ^3	−98	−71	−84	86	80	120	−104	155	96	81	−69	−89	−81	107

[a]Because of the absence of the amino (or carboxyamido) group in position 1 the angle φ is missing in the case of Mpa^1 and Cpp^1. The values of pseudo-ψ angles of this residue (in brackets) correspond to the C2-C2-C-N angle.

TABLE 7
SELECTED TORSION ANGLES OF THE CONFORMATIONS OF THE CYCLIC PART OF [Ths[1]]-AVP

		For the conformations shown in Fig. 3												
Energy (kcal/mol)		0.0	0.7	1.3	2.9	4.3	5.4	5.7	8.3	9.8	14.5	14.9	15.3	15.8	15.8
		Torsion angles (deg)													
Ths[1]	ψ	(−141)	(−145)	(129)	(−129)	(39)	(−44)	(88)	(−92)	(44)	(92)	(48)	(46)	(−104)	(56)
	χ^1	6	5	3	0	4	−6	0	−1	6	7	0	−6	−2	−0
	χ^2	118	134	−137	−103	51	−125	94	72	−119	71	168	−154	−152	143
	χ^3	−74	−74	99	84	88	88	−81	140	109	94	75	−112	78	80
Tyr[2]	φ	−95	−140	53	73	35	−51	−63	−76	−156	43	−171	173	−102	−164
	ψ	170	56	41	−58	73	−42	−26	80	78	40	119	90	−20	−171
Phe[3]	φ	−50	−147	−140	−150	73	−89	−79	−45	−34	58	50	51	−64	−52
	ψ	−41	173	179	173	−46	136	−6	−29	−45	28	33	35	−30	−43
Gln[4]	φ	−102	−53	−53	−51	−62	−53	−131	−56	−55	−81	53	63	−156	−93
	ψ	15	−38	103	−30	96	−36	−177	−36	−34	−162	31	6	174	116
Asn[5]	φ	−168	−75	59	−56	71	−92	−76	−103	−162	−74	−72	−84	−79	−59
	ψ	82	−20	29	−33	31	14	67	−35	45	73	−33	66	70	129
Cys[6]	φ	−112	−174	−133	−119	−164	−111	−79	−112	−65	−81	−84	−92	−64	−68
	ψ	97	109	103	90	143	109	121	91	121	118	115	113	124	123
	χ^1	−179	−173	−173	−179	77	174	−178	51	177	−51	−56	−50	−68	−73
	χ^2	80	−67	−98	−134	180	−122	178	99	79	−162	87	−46	100	66
	χ^3	−74	−74	99	84	88	88	−81	140	109	94	75	−112	78	80

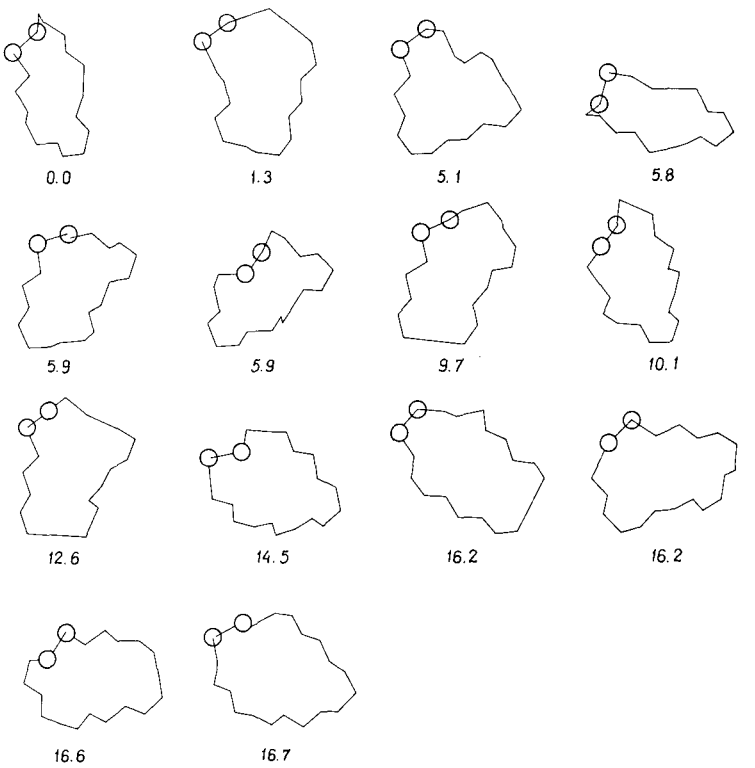

Fig. 2. Backbones of the cyclic parts of [Mpa^1]-OT, [Mpa^1]-AVP, and [Cpp^1]-AVP. Sulphurs are indicated with balls. Projections onto the mean planes of the 20-membered rings. The conformational energies are indicated below.

nated, because of the very low acidity of the guanidinium cation in water. Both Nikiforovich et al. [9] and Spasov and Popov [10] used a neutral guanidine group.

In the case of [Ths^1]-AVP, however, we also generated the starting points by attaching the benzene ring in position 1 to the lowest energy conformations of [Mpa^1]-AVP, which has led to structures of about 10 kcal/mol lower in energy when compared with those obtained by our 'standard' procedure, though similar as far as the geometry is concerned.

Some confirmation of our two-step computational procedure is that, when starting from purely initial (i.e., ring-closure corrected from Ref. 10) values of the torsion angles of [Mpa^1]-AVP, we have obtained a conformation of about 20 kcal higher in energy. Therefore, preoptimization of the geometry of the simplified cyclic parts prevented us from 'trapping' in the local minima, which arise when all the parts of a molecule are taken into account.

The conformations are in Figs. 4, 5, and 6. In Tables 8–10 are some selected torsion angles and parameters of the H-bonds formed.

RESULTS AND DISCUSSION

In this section, the conformations of the cyclic moieties of the compounds studied are analyzed

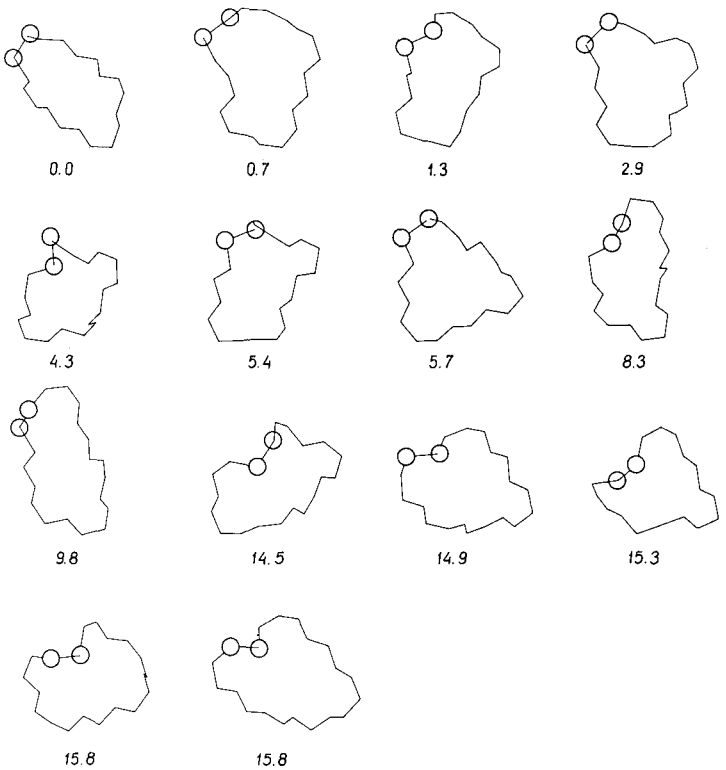

Fig. 3. Backbones of the cyclic parts of [Ths[1]]-AVP. Projections onto the mean planes of the 20-membered rings.

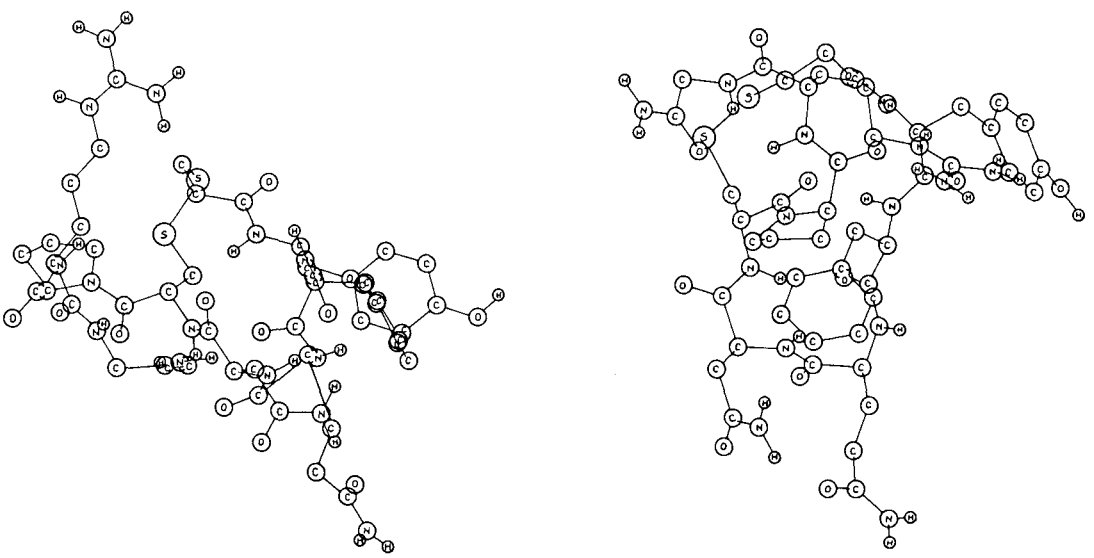

Fig. 4. Two lowest energy conformations of [Mpa[1]]-AVP (relative energy 0.0 and 2.3 kcal/mol) projected onto the mean plane of the 20-membered ring.

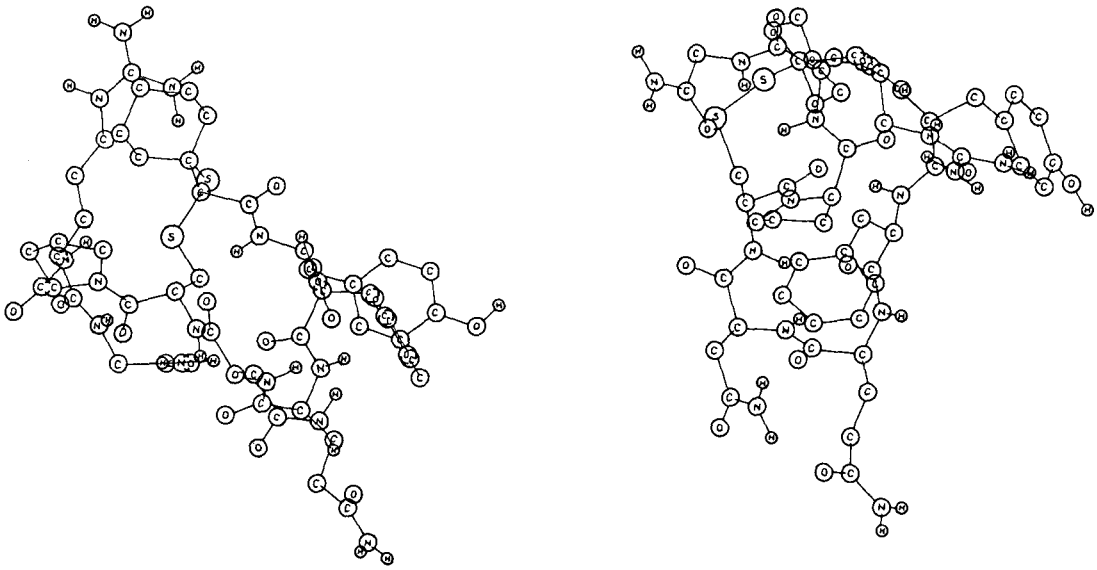

Fig. 5. Two lowest energy conformations of [Cpp^1]-AVP projected onto the mean plane of the 20-membered ring.

first, then those of the whole molecules of the vasopressin analogues. In the latter case, we also tried to correlate the conformational changes with the changes in their biological activity.

A model representation of the oxytocin and vasopressin ring

It is well-known that, in the case of such a complicated system as the oxytocin and vasopressin ring, the number of possible conformations is practically infinite (i.e., of the order of 10^{12}). Therefore we can hardly suppose that our calculations have covered all its low-energy conformations,

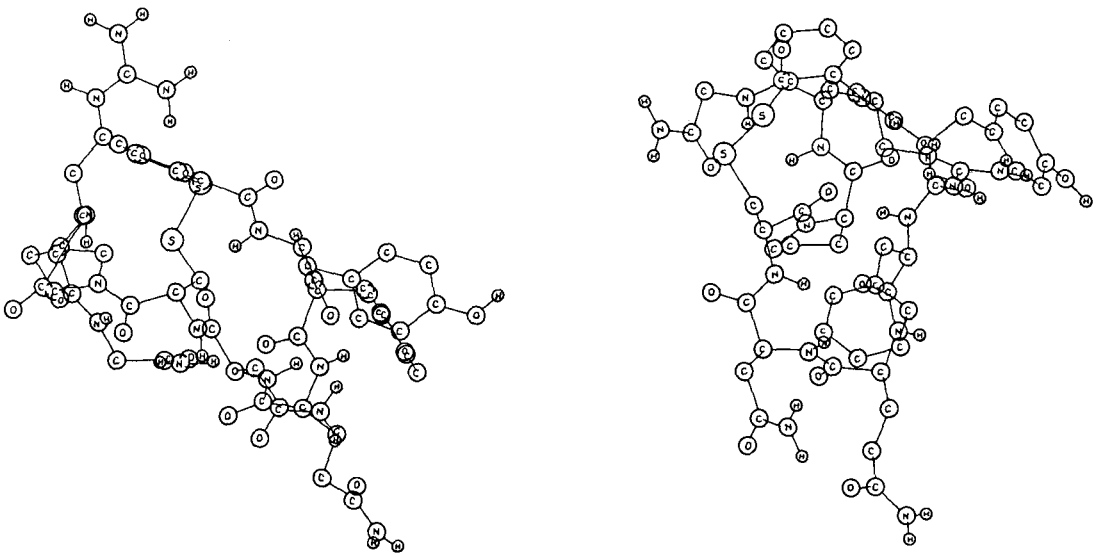

Fig. 6. Two lowest energy conformations of [Ths^1]-AVP projected onto the mean plane of the 20-membered ring.

TABLE 8
LOWEST ENERGY CONFORMATIONS OF [Mpa[1]]-AVP
(a) Selected torsion angles
Relative energies: 0.0 and 2.3 kcal/mol.

	φ	ψ	χ^1	χ^2	χ^3	χ^4
			(deg)			
Mpa[1]		(−167)	55	67	−78	
		(−90)	−62	174	−81	
Tyr[2]	−83	56	−176	−132	−179	
	−138	82	−165	−64	−23	
Phe[3]	52	−79	−178	66		
	−147	153	172	55		
Gln[4]	−64	−54	174	−170	−112	
	−42	−49	−180	−173	−105	
Asn[5]	−89	55	−61	92		
	−111	28	−56	109		
Cys[6]	−121	125	171	110	−78	
	−171	74	−164	−68	−81	
Pro[7]	−51	−37	−29	37		
	−69	−42	25	−36		
Arg[8]	−65	−20	−57	174	−179	132
	−147	−55	−70	78	179	105
Gly[9]	123	59				
	−84	159				

(b) Parameters of the hydrogen bonds[a]

Groups involved	X...Y distance (Å)	X-H...Y angle (deg)
Conformation 1		
N-H(Tyr[2]) .....O-C(Asn[5])	2.771	151.9
N-H(Phe[3]) .....O-C(Mpa[1])	2.853	151.0
N-H(Gln[4]).....O-C(Phe[3])	2.648	119.1
N-H(Asn[5]).....O-C(Tyr[2])	2.805	149.4
N-H(Cys[6]) .....O-C(Gln[4])	2.885	149.7
N-H(Gly[9]) .....O-C(Cys[6])	2.803	158.0
N′-H(Gly[9]) .....O-C(Phe[3])	2.818	158.1
N′-H(Gly[9]) .....O-C(Cys[6])	2.797	151.8
$CONH_2$(Asn[5]) .....$OCNH_2$(Gln[4])	2.775	140.9
N-H(Arg[8]).....S(Cys[6])	3.461	132.3
N2-H3(Arg[8]) .....S(Mpa[1])	3.182	146.0
Conformation 2		
N-H(Phe[3]) .....O-C(Phe[3])	2.725	95.7
N-H(Phe[3]) .....O-C(Cys[6])	2.730	148.9
N-H(Cys[6]) .....O-C(Phe[3])	2.888	158.2
N-H(Arg[8]).....O-C(Gly[9])	3.380	151.5
N′-H(Gly[9]) .....S(Cys[6])	3.381	116.2
$CONH_2$(Asn[5]) .....$OCNH_2$(Gln[4])	2.772	145.3
N2-H3(Arg[8]) .....H-O(Tyr[2])	2.739	171.1
N2-H3(Arg[8]) .....O-C(Pro[7])	2.629	174.5

[a]The criterion of the X-H...Y hydrogen bond was the H...Y distance less than 2.5 Å in case of Y = O or 3.0 Å in case of Y = S and the X-H...Y angle greater than 90°.

TABLE 9
LOWEST ENERGY CONFORMATIONS OF [Cpp[1]]-AVP
(a) Selected torsion angles
Relative energies: 0.0 and 2.0 kcal/mol.

	φ	ψ	χ^1	χ^2	χ^3	χ^4
			(deg)			
Cpp^1		(−170)	54	67	−80	
		(−87)	−61	174	−85	
Tyr^2	−82	55	−176	−134	−179	
	−137	83	−165	−63	−23	
Phe^3	52	−79	−178	64		
	−148	153	173	55		
Gln^4	−64	−54	174	−170	−110	
	−42	−49	180	−173	−108	
Asn^5	−89	52	−60	92		
	−111	28	−56	108		
Cys^6	−115	119	171	106	−80	
	−171	76	−167	−69	−85	
Pro^7	−50	−35	−30	37		
	−68	−44	25	−35		
Arg^8	−68	−20	−54	175	−175	137
	−147	−55	−70	78	179	102
Gly^9	127	60				
	−83	158				

(b) Parameters of the hydrogen bonds[a]

Groups involved	X...Y distance (Å)	X-H...Y angle (deg)
Conformation 1		
N-H(Tyr^2) .....O-C(Asn^5)	2.773	151.0
N-H(Phe^3) .....O-C(Mpa^1)	2.837	151.2
N-H(Gln^4) .....O- C(Phe^3)	2.649	119.3
N-H(Asn^5).....O-C(Tyr^2)	2.795	148.1
N-H(Cys^6) .....O-C(Gln^4)	2.911	149.8
N-H(Gly^9) .....O-C(Cys^6)	2.797	158.0
N′-H(Gly^9) .....O-C(Phe^3)	2.827	159.7
N′-H(Gly^9) .....O-C(Cys^6)	2.787	149.7
$CONH_2$(Asn^5) .....$OCNH_2$(Gln^4)	2.773	140.9
N-H(Arg^8) .....S(Cys^6)	3.469	131.4
N2-H3(Arg^8) .....S(Cpp^1)	3.180	144.2
Conformation 2		
N-H(Phe^3) .....O-C(Gln^4)	2.733	95.8
N-H(Phe^3) .....O-C(Cys^6)	2.724	148.5
N-H(Cys^6) .....O-C(Phe^3)	2.897	157.8
N-H(Arg^8).....O-C(Gly^9)	3.379	150.4
N′-H(Gly^9) .....S(Cys^6)	3.358	116.3
$CONH_2$(Asn^5) .....$OCNH_2$(Gln^4)	2.769	145.0
N2-H3(Arg^8) .....O-H(Tyr^2)	2.793	171.5
N2-H3(Arg^8) .....O-C(Pro^7)	2.689	173.9

[a]See footnote in Table 8.

TABLE 10
LOWEST ENERGY CONFORMATIONS OF [Ths¹]-AVP
(a) Selected torsion angles
Relative energies: 0.0 and 7.9 kcal/mol.

	φ	ψ	χ^1	χ^2	χ^3	χ^4
			(deg)			
Ths¹		(−133)	4	102	−74	
		(−124)	−3	131	−96	
Tyr²	−86	52	−173	−139	−179	
	−145	81	−164	−64	−23	
Phe³	53	−77	−178	65		
	−154	158	172	57		
Gln⁴	−64	−54	174	−169	−106	
	−41	−48	−180	−173	−105	
Asn⁵	−89	51	−60	91		
	−109	25	−58	108		
Cys⁶	−113	115	173	94	−74	
	−170	78	−161	−67	−96	
Pro⁷	−50	−52	−30	37		
	−71	−43	26	−36		
Arg⁸	−71	8	−45	175	−177	132
	−144	−51	−73	76	−179	105
Gly⁹	128	61				
	−107	164				

(b) Parameters of the hydrogen bonds[a]

Groups involved	X...Y distance (Å)	X-H...Y angle (deg)
Conformation 1		
N-H(Tyr²) .....O-C(Asn⁵)	2.794	146.8
N-H(Phe³) .....O-C(Ths¹)	2.898	150.4
N-H(Gln⁴) .....O-C(Tyr²)	2.633	121.3
N-H(Asn⁵) .....O-C(Tyr²)	2.786	148.5
N-H(Cys⁶) .....O-C(Gln⁴)	2.925	149.5
N-H(Arg⁸) .....S(Cys⁶)	3.127	98.8
N-H(Gly⁹) .....O-C(Cys⁶)	2.798	157.9
N′-H(Gly⁹) .....O-C(Phe³)	2.830	158.5
N′-H(Gly⁹) .....O-C(Cys⁶)	2.778	148.3
$CONH_2$(Asn⁵) .....$OCNH_2$(Gln⁴)	2.771	140.1
N2-H3(Arg⁸) .....S(Ths¹)	3.126	149.3
Conformation 2		
N-H(Phe³) .....O-C(Phe³)	2.680	99.6
N-H(Phe³) .....O-C(Cys⁶)	2.735	148.3
N-H(Cys⁶) .....O-C(Phe³)	2.871	159.8
$CONH_2$(Asn⁵) .....$OCNH_2$(Gln⁴)	2.772	144.9
N2-H3(Arg⁸) .....O-H(Tyr²)	2.791	171.1
N2′-H3(Arg⁸) .....O-C(Pro⁷)	2.691	174.0

[a]See footnote in Table 8.

although we started from the structures obtained by Spasov and Popov with the use of a physically and 'biochemically' reasonable procedure [5]. However, on the basis of the results obtained, we can try to answer the question as to whether, in the case of this relatively small and regular peptide system, there is any kind of symmetry which would help in a further, more detailed examination of the conformational space.

First, we decided to apply a 'reductionistic' approach which is commonly used in the case of peptide geometry and means simply considering only the positions of the α-carbons, assuming that virtual bonds exist between them. Such a construction can be considered as the *shape* of a peptide [25]. In contrast to real conformations, only the 'bond lengths' are constant here due to the rigidity of the peptide bond. The 'bond angles' should be only from a certain interval, approximately between 70° and 145°, in order to satisfy the real bond angle constraints at the α-carbons. Generally, a particular shape corresponds to an infinite number of geometries of a peptide, because there is an infinite number of possibilities for positioning the peptide bonds between them. On the other hand, however, it can be presupposed that certain shapes will include families of conformations which are energetically unfavourable, while other shapes include low-energy conformations. In practice, the assumption that the energy first of all depends on the configuration of the α-carbons is made when determining the backbone conformations of larger proteins. Each residue is thus represented by one or two pseudoatoms [24].

There are various possibilities for describing the shapes. A very interesting approach which is based on differential geometry, has been given by Rackovsky and Scheraga [26,27]. The authors have defined the curvature and the torsion of a peptide chain at each α-carbon, except for the first and two last ones. These values are strictly connected with the 'valence' and 'dihedral' angles of a shape, although concentrated in certain regions. In the case of large peptides, it makes it possible to distinguish the regions of β-turns, helical structures, etc., as well as the comparison of different conformations.

Other formalism has been introduced by Popov [25]. Each shape is denoted by a binary code, which is constructed by considering the dihedral angles between the α-carbons. If the absolute value of the dihedral angle involving α-carbons of residues of numbers i, i+1, i+2, and i+3 is greater than 90°, the letter e is assigned to the *i*th residue, which stands for the extended-type configuration of the residues i to i+2, otherwise the letter f is assigned (a folded-type configuration). The interactions between the residues i to i+3 are weak in the case of the extended- and strong in the case of the folded-type configurations. The whole code is simply the sequence of letters corresponding to the consecutive residues. Of course, such a binary code does not uniquely describe a shape. For example, the structures of which the first one is a helix and the second consists of subsequent + and − γ-turns are to be denoted by the same sequence of the letter f. It should be noted that, in these cases, even the local interactions (i.e., those within four neighbouring residues) are different.

We have built up the shapes of the cyclic parts of the oxytocin and vasopressin analogues by consequently linking all the α-carbons, including the link between the first and last residue as well. As a result, six-membered rings have been obtained.

For the reasons presented above, as far as the energy is concerned, it seems convenient to consider the conformational space of a peptide as a Cartesian product of two spaces, the first one being the space of the shapes, and the second one the space of certain internal arrangements of the peptide residues within a shape. The problem is only to find suitable bases of both spaces. As we

have already mentioned, we tried to find some quasi-symmetry of the vasopressin and oxytocin ring. We thought it interesting, therefore, to try to describe their shapes in terms of the cyclohexane geometries.

To achieve this, we calculated the 'internal coordinates' of the six-membered rings obtained from the calculated conformations of the cyclic parts of [Mpa^1]-OT, [Mpa^1]-AVP, [Cpp^1]-AVP, and [Ths^1]-AVP. They are summarized in Tables 11 and 12. As shown, all the pseudobonds crossing a peptide bond (α-carbon to α-carbon) are of an almost constant length of 3.8 Å. The 'bond' which links Mpa^1, Cpp^1 or Ths^1 and Cys^6 is of a much less stable length, because the disulphide fragment has at least four degrees of freedom, while the peptide bond is almost rigid. The 'valence angles' vary from about 65° to about 140°, usually being near 90–100°. However, in almost all the cases, the projection of a ring onto its mean plane is a convex hexagon (see Figs. 7 and 8). This supports the validity of using the cyclohexane geometries code as the basis of the analysis.

It is well-known that for cyclohexane three strainless structures can be distinguished: a *chair*, which is the global minimum; a *twist*, which is a local minimum; and a *boat*, a local maximum. Apart from these, there is an infinite number of strained structures of which the *sofa* structure is often distinguished, as it is the energy maximum in conformational transitions. These four structures have been taken as a basis of our analysis.

In our case the number of structures to be distinguished is greater, because all the atoms of the ring are different and therefore there is no permutational symmetry. It can easily be shown that there are two different chairs, six twists and boats, and 12 sofas. As the characteristics of the struc-

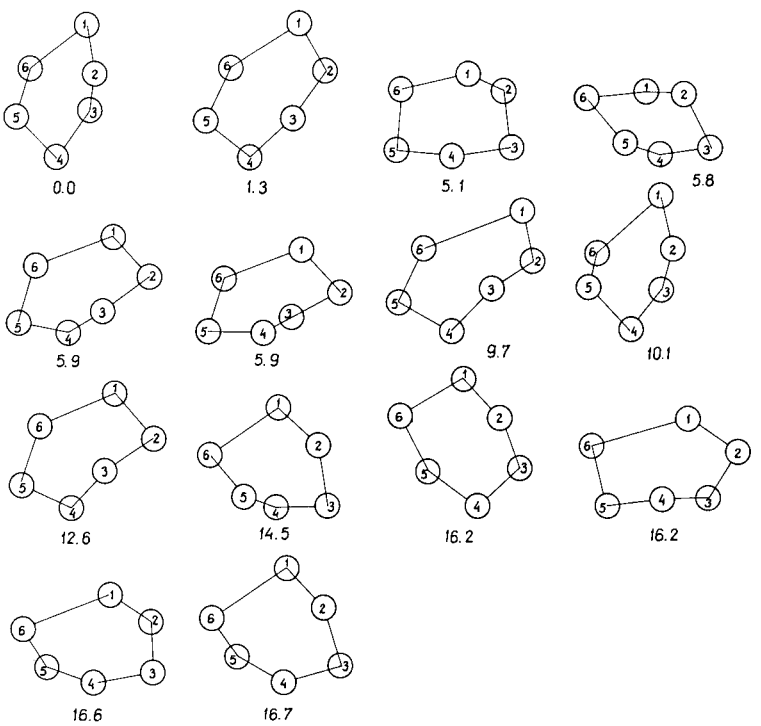

Fig. 7. Projections of the shapes of [Mpa^1]-OT, [Mpa^1]-AVP and [Cpp^1]-AVP onto the mean plane of the six-membered rings. Residue numbers are indicated.

TABLE 11
INTERNAL COORDINATES OF THE SHAPES OF THE CYCLIC PARTS OF [Mpa^1]-OT, [Mpa^1]-AVP AND [Cpp^1]-AVP

No.	Energy (kcal/mol)	Internal coordinates[a]						Shape code
		Mpa^1 (Cpp^1)	Tyr^2	Phe^3 (Ile^3)	Gln^4	Asn^5	Cys^6	
1	0.0	4.56	3.77	3.84	3.84	3.81	3.82	
		125.5	71.3	90.8	101.6	89.9	98.4	T_2^-
		−78	15	57	−139	51	22	
2	1.3	5.34	3.49	3.82	3.83	3.82	3.85	
		136.1	81.2	109.2	138.6	90.9	93.3	C_1^+
		−69	62	−37	97	−94	46	
3	5.1	4.73	3.75	3.82	3.83	3.82	3.81	
		108.3	99.9	91.2	94.9	143.3	88.6	T_1^-
		2	67	−94	49	44	−72	
4	5.8	4.24	3.74	3.81	3.84	3.83	3.81	
		69.1	101.0	96.5	83.1	90.2	105.8	T_1^+
		−33	−53	113	−20	−53	127	
5	5.9	5.79	3.82	3.81	3.82	3.83	3.84	
		117.4	96.8	90.4	117.7	90.5	89.9	T_3^-
		2	−61	18	58	−141	53	
6	5.9	6.06	3.84	3.84	3.84	3.83	3.82	
		105.7	95.4	88.4	93.1	92.7	86.6	T_3^+
		−15	69	−5	−66	155	−47	
7	9.7	6.68	3.83	3.81	3.80	3.82	3.84	
		136.1	79.2	86.3	129.9	106.8	91.2	S_6^+
		12	24	−41	146	−98	0	
8	10.1	5.91	3.42	3.83	3.83	3.82	3.82	
		94.4	67.5	121.0	97.8	89.7	97.8	T_2^-
		−93	50	36	−129	60	26	
9	12.6	5.39	3.77	3.83	3.81	3.80	3.81	
		128.7	104.4	85.5	127.3	91.3	97.0	T_3^-
		−3	−29	−1	93	−136	38	
10	14.5	5.29	3.81	3.84	3.85	3.84	3.81	
		88.5	98.4	130.2	87.6	89.3	89.3	T_1^+
		−65	2	46	−9	−71	136	
11	16.2	4.75	3.82	3.83	3.82	3.84	3.82	
		92.1	94.3	120.1	96.4	98.5	148.2	C_1^-
		45	−37	85	−96	48	−54	
12	16.2	6.39	3.75	3.84	3.83	3.82	3.82	
		90.6	129.9	90.4	94.3	115.6	99.1	S_1^+
		13	12	16	−52	138	−93	
13	16.6	6.00	3.56	3.82	3.82	3.81	3.82	
		78.0	123.0	98.0	95.7	137.5	96.0	B_3^+
		55	−8	−62	51	20	−106	
14	16.7	6.22	3.60	3.84	3.81	3.81	3.80	
		74.2	89.2	141.3	88.5	122.2	106.0	C_1^-
		83	−64	70	−59	48	−104	

[a]For the ith α-carbon, the corresponding column contains $d_{i,i-1}$ 'bond length', $\alpha_{i,i-1,i-2}$ 'bond angle', and $\beta_{i,i-1,i-2,i-3}$ torsion angle. In case of the Mpa^1 residue i−1 is the 6th α-carbon, etc.

TABLE 12
INTERNAL COORDINATES OF THE SHAPES OF THE CYCLIC PARTS OF [Ths[1]]-AVP

No.	Energy (kcal/mol)	Internal coordinates						Shape code
		Ths[1]	Tyr[2]	Phe[3]	Gln[4]	Asn[5]	Cys[6]	
1	0.0	3.65	3.73	3.83	3.82	3.83	3.80	
		97.5	89.4	128.5	94.0	95.6	118.8	T_2^-
		−97	44	33	−91	34	34	
2	0.7	5.00	3.63	3.82	3.83	3.83	3.85	
		127.7	83.7	104.7	140.6	91.0	92.2	C_1^+
		−83	77	−41	87	−85	51	
3	1.3	4.87	3.80	3.81	3.83	3.82	3.82	
		146.6	87.1	93.4	141.4	102.4	87.9	T_2^+
		64	−18	−37	101	−47	−25	
4	2.9	4.68	3.73	3.83	3.84	3.83	3.83	
		124.5	102.8	91.6	140.1	88.8	88.2	T_1^+
		−45	−31	44	−1	−81	73	
5	4.3	5.58	3.83	3.84	3.84	3.81	3.83	
		78.5	84.7	96.2	90.9	98.4	93.1	T_3^+
		−50	115	−31	−42	114	−21	
6	5.4	4.91	3.78	3.80	3.83	3.83	3.84	
		120.4	103.0	89.2	113.8	92.5	91.7	T_3^-
		14	−66	16	63	−128	46	
7	5.7	5.10	3.68	3.83	3.83	3.82	3.82	
		108.4	86.7	90.9	90.8	140.0	90.1	T_1^-
		4	64	−101	62	38	−70	
8	8.3	6.27	3.57	3.82	3.83	3.82	3.83	
		107.4	65.2	91.2	92.4	86.3	98.1	T_2^-
		−66	14	47	−167	75	17	
9	9.8	5.74	3.81	3.83	3.83	3.83	3.83	
		129.1	54.0	106.8	94.7	91.7	110.1	T_1^+
		−30	−7	74	−161	65	−10	
10	14.5	5.74	3.81	3.83	3.82	3.83	3.82	
		111.1	114.5	91.2	95.3	121.8	87.7	B_1^+
		−14	37	17	−68	133	−54	
11	14.9	5.99	3.82	3.83	3.84	3.83	3.82	
		86.0	91.4	129.0	87.4	88.8	91.2	T_1^+
		−59	−6	57	−19	−74	139	
12	15.3	5.87	3.84	3.83	3.85	3.84	3.80	
		92.8	83.2	120.6	88.0	89.6	87.7	T_1^+
		−53	−18	76	−37	−69	130	
13	15.8	5.76	3.71	3.84	3.82	3.81	3.82	
		90.5	106.6	97.0	90.6	139.1	93.4	B_3^+
		57	−10	−69	77	−10	−76	
14	15.8	5.95	3.78	3.84	3.80	3.81	3.82	
		71.4	95.6	141.5	89.0	107.1	111.3	C_1^-
		90	−49	56	−58	55	−121	

tures, we have chosen the ratios of the internal torsion angles. They are summarized in Table 13. Each shape is denoted by a shape letter code (C for a chair, T for a twist, B for a boat, and S for a sofa), a subscript which indicates how many subsequent permutations have been performed on a reference structure marked with 1, and a sign '+' or '−' which show whether the signs of the torsion angles have been inverted. These permutations and the sign changing are the 'symmetry

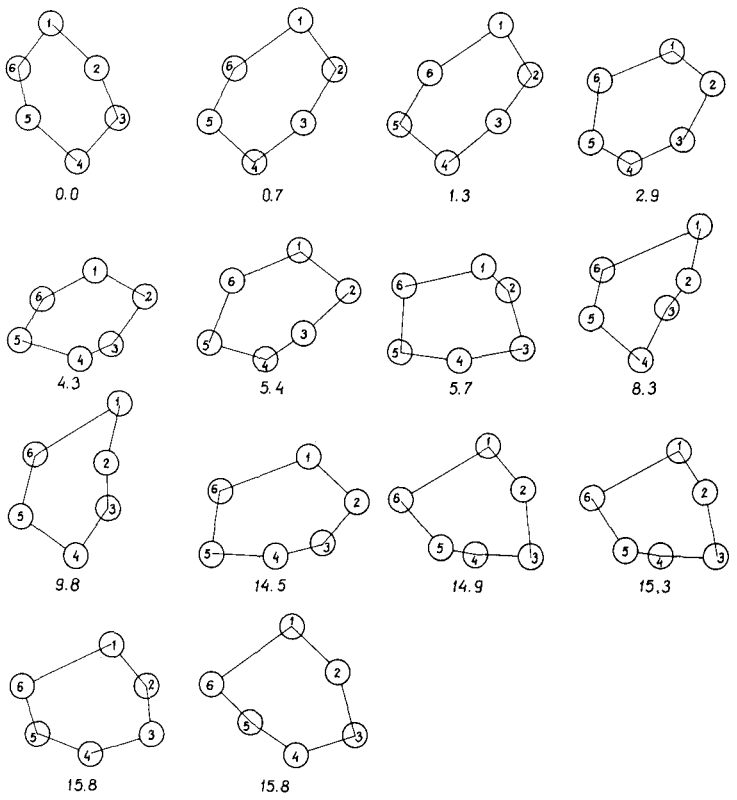

Fig. 8. Projections of the shapes of [Ths^1]-AVP onto the mean planes of the six-membered rings.

relations' between the structures. According to them the space of the 'ideal' shapes is split into four equivalence classes.

According to Table 13 we have classified the conformations of the cyclic parts of [Mpa^1]-AVP and [Ths^1]-AVP. In some cases it was hard to decide about the proper shape. Obviously, it could be assumed that a shape is a linear combination of some basis shapes, which would make the as-

TABLE 13
SIGNATURES OF THE INTERNAL TORSION ANGLES OF THE SHAPES OF THE VASOPRESSIN RING

Twists							Boats							Chairs							Sofas						
−1	−1	2	−1	−1	2	T_1^+	−1	1	0	−1	1	0	B_1^+	−1	1	−1	1	−1	1	C_1^+	0	0	1	−1	1	−1	S_1^+
1	1	−2	1	1	−2	T_1^-	1	−1	0	1	−1	0	B_1^-	1	−1	1	−1	1	−1	C_1^-	0	0	−1	1	−1	1	S_1^-
2	−1	−1	2	−1	−1	T_2^+	0	−1	1	0	−1	1	B_2^+								−1	0	0	1	−1	1	S_2^+
−2	1	1	−2	1	1	T_2^-	0	1	−1	0	1	−1	B_2^-								1	0	0	−1	1	−1	S_2^-
−1	2	−1	−1	2	−1	T_3^+	1	0	−1	1	0	−1	B_3^+								1	−1	0	0	1	−1	S_3^+
1	−2	1	1	−2	1	T_3^-	−1	0	1	−1	0	1	B_3^-								−1	1	0	0	−1	1	S_3^-
																					−1	1	−1	0	0	1	S_4^+
																					1	−1	1	0	0	−1	S_4^-
																					1	−1	1	−1	0	0	S_5^+
																					−1	1	−1	1	0	0	S_5^-
																					0	1	−1	1	−1	0	S_6^+
																					0	−1	1	−1	1	0	S_6^-

signment unambiguous. However, we did not think it worthwhile at the time. The results are given in Tables 11 and 12.

As shown, for both [Mpa^1]-AVP and [Ths^1]-AVP, the conformations definitely lowest in energy have the shapes T_2^- and C_1^+. On the other hand, the conformations of C_1^- shape (two in the case of [Mpa^1]-AVP and one in the case of [Ths^1]-AVP) are the highest in energy. In these extreme cases there was no ambiguity in deciding about the shapes.

It should be noted that according to the angles φ and ψ, the lowest energy conformations of the cyclic parts of [Mpa^1]-AVP and [Ths^1]-AVP are very different, the angles even having different signs (see Tables 8–10). Also, their projections onto the mean planes look different. Moreover, in the case of [Mpa^1]-AVP the resultant conformation is, with regard to the angles φ and ψ, different from the starting one, which on the other hand has the same shape T_2^-.

The internal coordinates of the shapes of the cyclic parts of the whole molecules are summarized in Table 14. As shown, the shape types have not changed after attaching the remaining parts of the molecules. We can therefore say that our shape code is the least changeable characteristic of the oxytocin and vasopressin ring. Moreover, owing to the good shape-energy correlation found already, we can conclude that the analysis of the conformations of this system in terms of the 'cyclohexane' shapes, including those which were not found among the conformations obtained in this work with the use of the 'standard' initial guesses, would probably shed new light on its conformational space and even the conformational transitions.

Analysis of the vasopressin analogues

As shown in the figures and tables, the lowest energy conformations of [Mpa^1]-AVP and [Cpp^1]-AVP are very similar. They have been generated from the same conformations of the cyclic part. Apart from the disulphide region which is mostly affected by the presence of the planar benzene ring, the conformations of [Ths^1]-AVP are also very similar. In each case the lowest energy conformation has a T_2^- shape as far as the ring moiety is concerned, and the second one – a C_1^+ shape.

As shown (see Tables 8–10), in all cases the first type conformations possess a distorted type II′ β-turn in the Phe^3-Gln^4 region, a type III β-turn in the Pro^7-Arg^8 region, and three γ-turns at Tyr^2, Phe^3 and Asn^5, respectively. The number of annular H-bonds is therefore very great (see Table 8b). In particular, two H-bonds can be distinguished between N-H(Tyr^2) and O-C(Asn^5), and N-H(Asn^5) and O-C(Tyr^2). The presence of the first has already been postulated by Urry and Walter in their first model of the oxytocin conformation [28]. In the case of C_1^+ type conformations there is a type I β-turn in the Gln^4-Asn^5 region, i.e., it is shifted one residue forward when compared with the T_2^- structure. The annular H-bonds are also shifted and occur between Phe^3 and Cys^6.

A very important feature of both types of conformation are strong interactions involving the side chains. In all cases there is a H-bond between the Asn^5 and Gln^4 side chains. In the first structure the charged guanidine group of arginine forms a H-bond with Cys^6 sulphur, while for the second type a H-bond between a guanidine hydrogen and phenol oxygen is present in interactions which have been reported neither by Nikiforovich et al. [9] nor by Spasov and Popov [10] who carried out the calculations on vasopressin. The reason is probably that they assumed a neutral instead of protonated guanidine group. On the other hand, the role of the interactions involving the charged guanidine group found in this work may be exaggerated, because in the real environment the guanidinium group becomes easily solvated.

It can also be noted that the energy difference between conformations is greatest in the case of [Ths^1]-AVP, a feature which has not been observed in the case of the cyclic parts conformation. This, together with the realization of the important role of the interactions involving the side chains, leads to a conclusion that these interactions are remarkably affected by the strains due to the benzene ring. These strains also emerge when comparing the *absolute* molecular mechanics energies of the analogues studied. Obviously, such comparison must be made bearing in mind that one does not compare the whole energy of these different molecules which is obviously not in-

TABLE 14

(A) INTERNAL COORDINATES OF THE SHAPES OF [Mpa^1]-AVP

No.	Energy (kcal/mol)	Internal coordinates						Shape code
		Mpa^1	Tyr^2	Phe^3	Gln^4	Asn^5	Cys^6	
1	0.0	3.35	3.81	3.86	3.11	2.98	3.80	
		107.8	83.8	89.3	64.1	124.5	90.0	T_2^-
		−78	27	59	−118	62	11	
2	2.3	5.70	3.80	3.80	3.84	3.81	3.84	
		143.8	74.8	104.0	141.8	90.8	96.2	C_1^+
		−52	60	−38	122	−102	30	

(B) INTERNAL COORDINATES OF THE SHAPES OF [Cpp^1]-AVP

No.	Energy (kcal/mol)	Internal coordinates						Shape code
		Cpp^1	Tyr^2	Phe^3	Gln^4	Asn^5	Cys^6	
1	0.0	3.28	3.81	3.86	3.83	3.81	3.80	
		110.7	81.4	89.7	94.5	89.5	89.8	T_2^-
		−111	28	59	−112	25	47	
2	2.0	5.76	3.80	3.80	3.84	3.81	3.84	
		143.1	74.6	103.9	142.2	91.1	96.1	C_1^+
		−52	60	−38	123	−102	30	

(C) INTERNAL COORDINATES OF THE SHAPES OF [Ths^1]-AVP

No.	Energy (kcal/mol)	Internal coordinates						Shape code
		Ths^1	Tyr^2	Phe^3	Gln^4	Asn^5	Cys^6	
1	0.0	3.70	3.80	3.86	3.83	3.81	3.80	
		107.0	76.2	93.8	94.2	88.4	89.1	T_2^-
		−115	32	55	−118	27	45	
2	7.9	5.47	3.79	3.80	3.84	3.81	3.84	
		144.0	74.3	107.3	141.7	91.0	96.7	C_1^+
		−59	64	−40	111	−92	32	

cluded in the molecular mechanics, but merely the nonbonded and strain energy. In the case of [Cpp^1]-AVP, the energy is approximately the same as for the same conformations of [Mpa^1]-AVP which means that the presence of the cyclohexane ring is negligible as far as the energy is concerned, while in the case of [Ths^1]-AVP, the energy is of about 6.8 kcal/mol higher in the case of T_2^- structure and of about 12.8 kcal/mol higher in the case of C_1^+ conformation.

When comparing our conformations of [Mpa^1]-AVP with the results of conformational calculations on AVP performed by Spasov and Popov, we can conclude that none of their three conformations of AVP is, according to the torsion angles, identical to ours. Particular differences arise in the Phe^3-Gln^4 region which in their calculations has in all cases a type III β-turn structure [10]. However, the analysis of the ring shapes of the three lowest energy conformations obtained by Spasov and Popov has revealed that the shapes are T_2^-, T_2^-, and T_1^-, respectively. Thus their lowest energy conformation has the same ring shape as ours.

It can also be noted that our C_1^+ shape conformation of the cyclic moiety of [Mpa^1]-AVP is very similar to the crystallographic conformation of the pressinoic acid [11]. On the other hand the crystallographic conformation of [Mpa^1]-OT [12] is very similar to our [Mpa^1]-AVP structure of T_2^- shape.

The only significant differences in the conformations of the three vasopressin analogues studied are between [Mpa^1]-AVP or [Cpp^1]-AVP and [Ths^1]-AVP and occur in the disulphide region. The disulphide bridge is thought to play an important role in both binding to the receptor and further biological reaction. Our calculations are in full agreement with this assumption. In the case of [Cpp^1]-AVP the bulky cyclohexyl ring near the disulphide bridge, although it does not change the hormone geometry in this region, enables merely the binding to the V_1 receptor to take place at the same time prohibiting the biological reaction. Therefore [Mpa^1]-AVP has high pressor activity, while [Cpp^1]-AVP having very similar conformational space is a strong antagonist of the pressor response. In the case of [Ths^1]-AVP substantial changes in the disulphide bridge environment must lead to a remarkable decrease in the affinity to the V_1 receptor which explains the absence of the pressor activity of this compound (see Table 15). Of course, the above considerations would

TABLE 15
BIOLOGICAL CHARACTERISTICS OF [Mpa^1]-AVP AND ITS ANALOGUES

Peptide	Pressor potency (U/mg)	Antipressor potency (pA_2)	Relative affinity to hepatic V_1 receptor	Antidiuretic potency (U/mg)	Relative affinity to renal V_2 receptor
AVP	360[a]		1[b]	323[a]	1[b]
[Mpa^1]-AVP	346[c]			1745[c]	
[Cpp^1]-AVP		8.35[d]	1.5[b]	0.033[d]	1/65[b]
[Ths^1]-AVP	0.04[e]		1/36[b]	0.12[e]	1/1200[b]

[a]Ref. 37.
[b]Ref. 17.
[c]Ref. 14.
[d]Ref. 15.
[e]Ref. 16.

be more complete if the change or at least the direction of the change of geometry on binding to the receptor were known.

Similar conclusions can be drawn analyzing the interactions of the compounds studied with the V_2 (antidiuretic) receptor. In this case, however, the data concerning both affinity to the receptor and biological activity indicate that introducing a bulky substituent near the disulphide region causes much greater perturbations, making the binding to the receptor more difficult.

ACKNOWLEDGEMENT

This work was supported by grants CPBR-3.13.4.3.2 and CPBP-05.06.1.5.4.

REFERENCES

1 Malon, P., In Jost, K., Lebl, M. and Brtnik F. (Eds.) CRC Handbook of Neurohypophyseal Hormone Analogs, Vol. 1, CRC Press, Boca Raton, FL, 1987, p.211.
2 Hempel, J.C., In Smith, C.W. (Ed.) The Peptides, Vol. 8, Academic Press, New York, 1987, pp. 209–237.
3 Van Gunsteren, W.F. and Berendsen, H.J.C., In Hermans, J. (Ed.) Molecular Dynamics and Protein Structure, Proceedings of a Workshop, 13–18 May, 1984, University of North Carolina, Polycrystal Book Service, P.O. Box 27, Western Springs, IL 60658, 1985, p. 5.
4 Nikiforovich, G.V., Leonova, V.I., Galaktionov, S.G. and Chipens, G.I., Int. J. Pept. Protein Res., 13, (1979) 363–373.
5 Spasov, V.Z. and Popov, E.M., Bioorg. Khim., 7 (1981) 24–44.
6 Momany, F.A., McGuire, R.F., Burgess, A.W. and Scheraga, H.A., J. Phys. Chem., 79 (1975) 2361–2381.
7 Dashevskii, V.G., Conformations of Organic Molecules (in Russian), 'Khimiya', Moscow, 1974.
8 Deslauriers, R., Smith, I.C.P. and Walter, R., Biochem. Biophys. Res. Commun., 48 (1972) 854–857.
9 Nikiforovich, G.V., Galaktionov, S.G. and Chipens, G.I., Conformations of Peptide Bioregulators (in Russian), Medicina, Moscow, 1983.
10 Spasov, V.Z. and Popov, E.M., Bioorg. Khim., 7 (1981) 502–514.
11 Blundell, T. and Wood, S., Annu. Rev. Biochem., 51 (1982) 123–154.
12 Wood, S.P., Tickle, I.J., Trehorne, A.M., Prits, J.E., Mascarenhas, Y., Li, J.Y., Husoin, J., Cooper, S., Blundell, T.L., Hruby, V.J., Buken, A., Fischman, A.J. and Wyssbrod, H.P., Science, 232 (1986) 633–636.
13 Langs, D.A., Smith, G.D., Stezowski, J.J. and Hughes, R.E., Science, 232 (1986) 1240–1242.
14 Manning, M., Balaspiri, L., Moehring, J., Haldar, J. and Sawyer, W.H., J. Med. Chem., 19 (1976) 842–845.
15 Kruszynski, M., Lammek, B., Manning, M., Seto, J., Haldar, J. and Sawyer, W.H., J. Med. Chem., 23 (1980) 364–368.
16 Grzonka, Z., Lankiewicz, L., Kasprzykowski, F., Liwo, A. and Melin, P., In Theodoropoulos (Ed.) Peptides 1986, Walter de Gruyter, Berlin, 1987, pp. 493–496.
17 Fahrenholz, F. and Grzonka, Z., unpublished results.
18 Weiner, S.J., Kollman, P.A., David, A.C., Chandra Singh, U., Ghio, C., Alagona, G., Profeta, S. and Weiner, P., J. Am. Chem. Soc., 106 (1984) 765–784.
19 Allinger, N.L. and Yuh, Y.H., QCPE, Program No. 395, 1977.
20 Byrne, D. and Hall, C.A., Numerical Solution of Nonlinear Algebraic Equations, Academic Press, New York, 1970.
21 Hoffman, H.J. and Birner, P., Chem. Phys. Lett., 37 (1976) 608–610.
22 Parr, W.J.E. and Schafer, T., J. Magn. Reson., 25 (1977) 171–176.
23 Hummel, J.P. and Flory, P.J., Macromolecules, 13 (1980) 479–484.
24 Crippen, G.M. and Viswandhan, V.N., Int. J. Pept. Protein Res., 24 (1984) 273–296.
25 Popov, E.M., Int. J. Quantum Chem., 16 (1979) 707–737.
26 Rackovsky, S. and Scheraga, H.A., Macromolecules, 11 (1978) 1168–1174.
27 Rackovsky, S. and Scheraga, H.A., Macromolecules, 13 (1980) 1440–1453.
28 Urry, D.W. and Walter, R., Proc. Natl. Acad. Sci. U.S.A., 68 (1971) 956–958.
29 Blake, C.C.F. and Small, R.W.H., Acta Crystallogr., Sect. B,28 (1972) 2201–2206.

30 Flett M. St. C., Spectrochim. Acta, 18 (1962) 1537–1556.
31 Rao, C.N.R., Randhawa H.S. and Reddy N.V.R., Spectrochim. Acta, 32 (1976) 1537–1556.
32 Kniseley, R.N., Fassel V.A., Farquhar E.L. and Gray, L., Spectrochim. Acta 18 (1962) 1217–1230.
33 Green, J.H.S. and Harrison, D.J., Spectrochim. Acta, 33 (1977) 583–587.
34 Sacerdotti, M., Gilli, G. and Damaso, P., Acta Crystallogr., Sect. B,31 (1975) 327–329.
35 Cymerman, J. and Willis, J.B., J. Chem. Soc., (1951) 1332–1337.
36 Van Wart, H.E. and Scheraga, H.A., J. Phys. Chem., 80 (1976) 1812.
37 Manning, M., Coy, E.J., Sawyer, W.H. and Acosta, M., J. Med. Chem. 16 (1973) 463–466.

APPENDIX

A ring closure algorithm

Consider an n-membered ring beginning at atom number 1 and ending at atom number n. Assume that all the bond lengths and valence angles of the ring have given values. If the coordinates of the atoms are calculated starting from atom 1, they will depend neither on the 1 – n bond length nor on (n – 1) – n – 1 and n – 1 – 2 bond angles. Therefore using a certain set of torsion angles does not necessarily imply satisfying all the bond lengths and bond angle constraints. Assume that only the torsion angles are to be varied. Therefore, we can write the following three equations for the constraints:

$$\begin{aligned} d_{1,n} &= f_1(\beta_1, \beta_2, \ldots, \beta_m) \\ \alpha_{n-1,n,1} &= f_2(\beta_1, \beta_2, \ldots, \beta_m) \\ \alpha_{n,1,2} &= f_3(\beta_1, \beta_2, \ldots, \beta_m) \end{aligned} \tag{2}$$

or in the matrix notation:

$$\mathbf{f}(\boldsymbol{\beta}) - \mathbf{C} = \mathbf{0}$$

where m is the number of torsion angles to be varied, $m \leqslant n - 3$,

$\beta_1, \beta_2, \ldots, \beta_m$ are the variable torsion angles
$\boldsymbol{\beta} = [\beta_1, \beta_2, \ldots, \beta_m]^T$
$\mathbf{C} = [d_{1,n}, \alpha_{n-1,n,1}, \alpha_{n,1,2}]^T$
$\mathbf{f} = [f_1, f_2, f_3]^T$

Usually $m > 3$ and, therefore, this system has, in general, an infinite number of solutions. However, in practice, we are interested in the torsion angles which differ least from the initially assumed values. It can be achieved precisely by minimizing the sum of the squares of the differences between the initial and final torsion angles having assumed Eqs. (2) to hold. This leads to the Lagrange multipliers method. However, nearly the same solution can be obtained by applying Newton's method [20] to system (2) assuming that the increments in βs are in each iteration a linear combination of the gradient of f. This can be written as system (3).

$$\begin{aligned} \boldsymbol{\beta}^{<p+1>} &= \boldsymbol{\beta}^{<p>} + \Delta\boldsymbol{\beta}^{<p>} \\ \mathbf{f}_{\beta}(\boldsymbol{\beta}^{<p>}) &= \mathbf{C} - \mathbf{f}(\boldsymbol{\beta}^{<p>}) \\ \Delta\boldsymbol{\beta}^{<p>} &= \mathbf{f}_{\beta}^{T}(\boldsymbol{\beta}^{<p>})\, \mathbf{v}^{<p>} \end{aligned} \tag{3}$$

where p is the number of the iteration.

Based on (3), we can easily write down the Eqs. system (4), for the linear combination coefficients, $\mathbf{v}$.

$$\mathbf{f}_\beta(\boldsymbol{\beta}^{<p>})\mathbf{f}_\beta^{T}(\boldsymbol{\beta}^{<p>})\mathbf{v}^{<p>} = \mathbf{f}_\beta^{T}(\boldsymbol{\beta}^{<p>})\,(\mathbf{C} - \mathbf{f}(\boldsymbol{\beta}^{<p>})) \tag{4}$$

or $\mathbf{A}_\beta{}^{<p>}\mathbf{v}^{<p>} = \mathbf{B}^{<p>}$

The matrix A is of 3×3 dimension and in general has the full rank, which means that system (4) is solvable. It can be proved that if f is linear in β, this algorithm gives precisely the values of βs which are the closest to the initial ones. In our case, we have varied all the angles φ and ψ of the oxytocin and vasopressin ring. Instead of using the original Newton's method which is unstable when the starting approximation is far from the minimum, we have applied the more stable method of Marquardt [20]. The derivatives in the torsion angles were approximated by the divided differences. We have found the algorithm to converge reasonably, even in the case of [Ths^1]-AVP when the initial S-S bond length and the C-S-S bond angles differed very much from their correct values.